Novel Placido-derived Topography-guided Excimer Corneal Normalization With Cyclorotation Adjustment: Enhanced Athens Protocol for Keratoconus

Anastasios John Kanellopoulos, MD; George Asimellis, PhD

ABSTRACT

PURPOSE: To comparatively investigate the efficacy of the enhanced Athens Protocol procedure guided by novel Placido-derived topography with cyclorotation compensation (the cyclorotation adjusted group) to similar cases guided by Scheimpflug-derived tomography without cyclorotation compensation (the non-cyclorotation adjusted group).

METHODS: Two groups were evaluated: the cyclorotation adjusted group (n = 110 eyes) and the non-cyclorotation adjusted group (n = 110 eyes). Analysis was based on digital processing of Scheimpflug imaging derived curvature difference maps preoperatively and 3 months postoperatively. The vector (r, ϑ) corresponding to the steepest corneal point (cone) on the preoperative surgical planning map (r_p, ϑ_p) and on the curvature difference map (r_d, ϑ_d) were computed. The differences between the peak topographic angular data ($\Delta\vartheta = |\vartheta_p - \vartheta_d|$) and weighted angular difference ($W\Delta\vartheta = \Delta\vartheta \times \Delta r$) were calculated.

RESULTS: For the cyclorotation adjusted group, $\Delta\vartheta$ was 7.18° ± 7.53° (range: 0° to 34) and $W\Delta\vartheta$ was 3.43 ± 4.76 mm (range: 0.00 to 21.41 mm). For the non-cyclorotation adjusted group, $\Delta\vartheta$ was 14.50° ± 12.65° (range: 0° to 49°) and $W\Delta\vartheta$ was 10.23 ± 15.15 mm (range: 0.00 to 80.56 mm). The cyclorotation adjusted group appeared superior to the non-cyclorotation adjusted group, in both the smaller average angular difference between attempted to achieved irregular curvature normalization and in weighted angular difference, by a statistically significant margin ($\Delta\vartheta$: $P = .0058$; $W\Delta\vartheta$: $P = .015$).

CONCLUSIONS: This study suggests that employment of the novel Placido-derived topographic data of highly irregular corneas, such as in keratoconus, treated with topography-guided profile with cyclorotation compensation leads to markedly improved cornea normalization.

[*J Refract Surg.* 2015;31(11):768-773.]

Corneal cross-linking (CXL) is considered a valid option for progressive keratoconus/corneal ectasia treatment.[1] By increasing corneal biomechanical strength, CXL results in keratectasia arrest.[2] In addition, CXL has also been shown to improve corneal irregularity and reduce central anterior corneal steepening.[3]

Combined with CXL, partial anterior surface normalization via topography-guided customized partial excimer laser ablation may offer, in addition to keratectasia arrest, improved topographic and refractive outcomes.[3,4] The Athens Protocol comprises phototherapeutic keratectomy (PTK) of 50 µm, a partial photorefractive keratectomy (PRK) for the topography-guided customized anterior surface normalization, and high-fluence CXL for corneal stabilization.[5] Long-term results[6] and anterior segment optical coherence tomography quantitative findings[7] have demonstrated the stability of the procedure in large cohorts of patients. Variations of this technique have been applied and reported globally.[8-14]

Because the topography-guided ablation step of the procedure bears a high degree of customization, the impact of effective alignment between treatment planning based on the topography-derived data and surgically applied ablation pattern is pivotal for a successful outcome. Critical parameters affecting alignment are horizontal and vertical eye movements, eye pupil centroid shift, and possible cyclorotation. The significance of these principles has been reported preoperatively and intraoperatively in refractive procedures.[15] High-speed active eye tracking along with cyclorotational topographic adjustment (CTA) has been introduced during the past 2 years in refractive lasers such as the EX500 excimer laser (Alcon Laboratories, Inc., Fort Worth, TX), which

From Laservision.gr Clinical and Research Eye Institute, Athens, Greece (AJK); and NYU Medical School, Department of Ophthalmology, New York, New York (GA).

Submitted: April 28, 2015; Accepted: August 11, 2015

Dr. Kanellopoulos is a consultant for Alcon/WaveLight, Allegran, Avedro, and i-Optics. Dr. Asimellis has no financial or proprietary interest in the materials presented herein.

Correspondence: Anastasios John Kanellopoulos, MD, Laservision.gr Clinical and Research Eye Institute, 17 Tsocha Street, Athens, 115 21 Greece. E-mail: ajk@brilliantvision.com

doi: 10.3928/1081597X-20151021-06

is employed for the excimer ablation step of the Athens Protocol studied herein.

The enhanced Athens Protocol incorporates the above surgical device improvements and also introduces surgical procedure changes, specifically the choice of the Placido-derived topography data produced by a novel topographic device (Vario instead of the Oculyzer II Scheimpflug-derived tomography [Alcon Laboratories, Inc./WaveLight AG, Erlangen, Germany]) and the reversal of the two excimer laser ablation steps: PRK now precedes PTK.

The purpose of this study is to comparatively investigate the correlation between achieved and intended corneal topography changes when employing the novel CTA procedure in comparison to the previously developed technique (based on the available technology at that time) in which no cyclorotational adjustment was available.

PATIENTS AND METHODS

This retrospective comparative study received approval by the ethics committee of Laservision.gr Clinical and Research Eye Institute, Athens, Greece, and adhered to the tenets of the Declaration of Helsinki. Signed informed consent was obtained from the patients at the time of the first clinical visit.

Two hundred twenty consecutive eyes of 220 different patients who had the Athens Protocol were retrospectively investigated. Inclusion criteria were clinical diagnosis of progressive keratoconus, minimum age of 17 years, and a minimum corneal thickness of approximately 300 µm measured by anterior segment optical coherence tomography. All patients had completed an uneventful Athens Protocol and were observed for approximately 1 year. Exclusion criteria for the procedure were systemic disease, previous eye surgery, ocular chemical injury, a history of delayed epithelial healing, and pregnancy or lactation (female patients).

Two groups were evaluated: patients who had CTA (the cyclorotation adjusted group [n = 110 eyes]) and patients who did not have CTA (the non-cyclorotation adjusted group [n = 110 eyes]).

Common to both groups, the design of the ablation pattern (profile) was performed via the Aqua software of the Alcon Refractive Suite, which is part of the EX500 excimer laser. The imported topography-derived data (approximately four acquisitions usually selected from 10 to 30 actual individual acquisitions) were selected to improve the default statistical data provided by the planning software. Specifically, we tried to match images with consistent keratometries and cylinder axes, as well as reproducibility that would minimize the maximum deviation index to a value less than 0.1. This methodology aimed to select a group of topography images that were consistent and reproducible. In all cases, the neuro-tracking option was on. No manual marking was used in either group.

In both groups, the excimer laser ablation steps (employing the EX500 excimer laser) were applied with the following sequence (**Figure A**, available in the online version of this article):

1. Partial excimer laser PRK performed with the EX500 laser's topography-guided custom ablation treatment mode. A typical optical zone was 5 to 5.50 mm with a limit of 50 µm to be removed over the steepest/thinnest cornea point.
2. Excimer laser ablation (uniform 50 µm over a 7-mm zone) employing the PTK mode.

The enhanced Athens Protocol presented herein also stems from recently reported[16] optimized ablation profiles. Previously, the procedure employed the sequence as follows: the PTK step was performed first, followed by the PRK step.[6]

Following ablation, the cross-linking step of the procedure involved ultraviolet-A irradiance of 6 mW/cm^2, applied for 15 minutes employing the KXL system (Avedro Inc., Waltham, MA).

The differences between the two groups were the following. In the cyclorotation adjusted group, the surgical planning corneal topography data were derived from the novel Allegro Topolyzer Vario (Alcon Laboratories, Inc.), a wide-cone Placido corneal topographer.[17] CTA was based on infrared iris imaging data comparison between the Vario device and the EX500 imaging. On the EX500 excimer laser, the previously imported iris information data is compared to the live infrared image of the eye tracking system, and any detected cyclotortional change (detection threshold 0.5°) was statically compensated. The angle sign is positive for clockwise and negative for counter-clockwise rotation. The notation in this system was common for both eye lateralities (ie, does not follow the positive for excyclotorsion, corresponding to the upper pole of the eye rotating to the temporal side, and negative for incyclotorsion).

In the non-cyclorotation adjusted group, the surgical planning corneal imaging topography data were derived from the Oculyzer II, a Scheimpflug imaging device based on the Pentacam (Oculus Optikgeräte GmbH, Wetzlar, Germany). Cyclorotational topographic adjustment is not available with this system.

Data Collection and Analysis

The public domain, Java-based image processing software ImageJ (version 1.49; National Institutes of

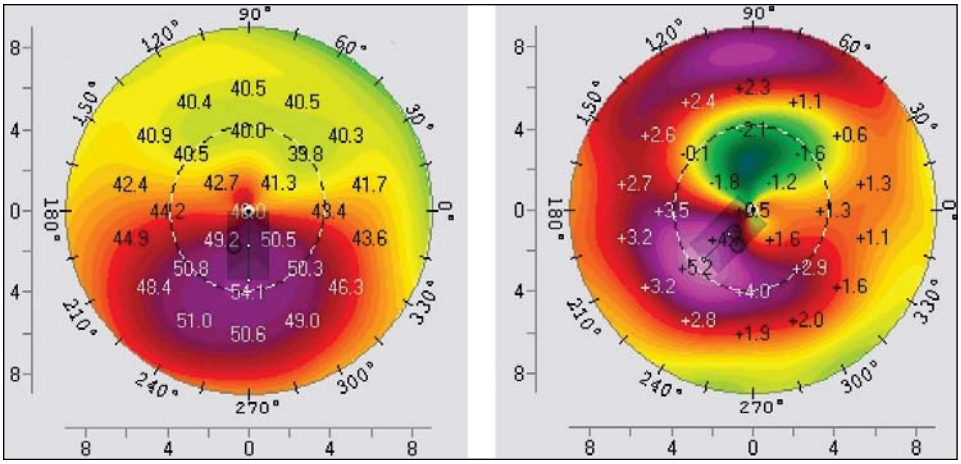

Figure 1. Measurement of axial and radial coordinates of the steepest corneal point with the ImageJ software (National Institutes of Health, Bethesda, MD) corresponding to (left) the preoperative map and (right) difference map. The preoperative map vector had the coordinates r_p = 1.69 mm, ϑ_p = 270°. The difference map vector had the coordinates, r_d = 1.69 mm, ϑ_d = 225°. There is evident difference between the two maps, which may be attributed to non-compensation of cyclorotation: the difference between the peak topographic angular data ($\Delta\vartheta$) and weighted angular difference ($W\Delta\vartheta$) corresponding to these data were 45° and 58.30 mm, respectively.

Health, Bethesda, MD)[18] was used to digitally process Scheimpflug-imaging data derived from the Pentacam HR. Specifically, the 'compare 2 exams' output from the Scheimpflug imaging device was analyzed. The output consists of three sagittal curvature images (**Figure B**, available in the online version of this article) consisting of the preoperative map, the postoperative map, and the difference (change) of the two maps. The first map corresponds to the planned ablation pattern, whereas the third map corresponds to the achieved ablation pattern.

Scheimpflug screening, an integral step of the Athens Protocol, was chosen to analyze both groups for the simple reason that the available software offers more data output options. Standardizing on one analysis device also helps eliminate potential bias in data evaluation.

Employing the straight line tool offered by ImageJ, we computed the vector (expressed in polar coordinates radius r, reported in pixels; and angle ϑ, reported in degrees) corresponding to the steepest (peak topographic) corneal point (cone) on the preoperative map (r_p, ϑ_p) and the difference map (r_d, ϑ_d) (**Figure 1**). The origin of each vector (r = 0, ϑ = 0) was the center of the curvature map. Pixels were converted to millimeters, based on the measured correspondence of the 9-mm diameter of the curvature maps to 254 pixels. Thus, the pixel data were converted to millimeters using the 1 pixel to 0.035 mm ratio. Due to the terminology in ImageJ, the lower hemicycle angles were reported as negative (range: 0° to -180°); to adjust for the Scheimpflug imaging terminology, the value of 360° was added to all negative angle data (lower hemicycle). Subsequently, we computed and subjected to analysis the following metrics:

1. $\Delta\vartheta$ is defined as the absolute angular difference between the peak topographic angular data: $\Delta\vartheta = |\vartheta_p - \vartheta_d|$. $\Delta\vartheta$ is expressed in degrees.
2. $W\Delta\vartheta = \Delta\vartheta \times \Delta r$ is defined as the weighted angular difference between the peak topographic data, where ϑr is the modulus of the difference between the two vectors: $\Delta r = |r_d - r_p|$. $W\Delta\vartheta$ is expressed in millimeters.

By virtue of their definition, an ideal treatment on an eye with zero cyclorotation corresponds to a zero $\Delta\vartheta$ and a zero $W\Delta\vartheta$. Realistically, however, there are always some deviations. In addition, due to the nature of the treatment, the postoperative cone location changes not only angularly, but also radially. This is why we also introduced the weighted angular difference, which accounts for both deviations.

Additional data employed in the study include visual acuity, thinnest corneal thickness, and topographic keratoconus classification, both Scheimpflug-imaging derived. Descriptive statistics and analysis were performed by Minitab (version 16.2.3; MiniTab Ltd., Coventry, United Kingdom). A *P* value less than .05 was considered statistically significant. Data are presented by mean ± standard deviation (minimum to maximum).

RESULTS

The 110 eyes (37 women and 73 men) included in the cyclorotation adjusted group included 53 right eyes and 57 left eyes. Mean patient age at the time of the operation was 25.7 ± 6.9 years (range: 18 to 44 years). Follow-up was 15.7 ± 10.5 months (range: 12 to 24 months). Preoperative uncorrected distance visual acuity was 0.19 ± 0.22 decimal (range: 0.001 to 0.7 decimal) and corrected distance visual acuity was 0.62 ± 0.24 decimal (range: 0.10 to 1.00 decimal). Preoperative thinnest corneal thickness was 441.87 ± 45.29 µm (range: 325 to 541 µm). One year postoperatively, uncorrected distance visual acuity was 0.53 ± 0.28 (range: 0.01 to 1.0), corrected distance visual acuity was 0.78 ± 0.25 (range: 0.25 to 1.00), and thinnest corneal thickness was 375.98 ± 63.12 µm (range: 302 to 498 µm).

The 110 eyes (41 females and 69 males) in the non-cyclorotation adjusted group included 60 right eyes and

50 left eyes. Mean patient age at the time of the operation was 25.2 ± 6.5 years (range: 18 to 38 years). Follow-up was 19.9 ± 12.1 months (range: 12 to 36 months). Preoperative uncorrected distance visual acuity was 0.18 ± 0.23 (range: 0.001 to 1.0) and corrected distance visual acuity was 0.63 ± 0.33 (range: 0.10 to 1.00). Preoperative thinnest corneal thickness was 448.11 ± 48.65 µm (range: 315 to 539 µm). One year postoperatively, uncorrected distance visual acuity was 0.59 ± 0.28 (range: 0.01 to 1.20), corrected distance visual acuity was 0.82 ± 0.19 (range: 0.20 to 1.25), and thinnest corneal thickness was 363.13 ± 55.43 µm (range: 298 to 487 µm).

Both groups were matched for age, gender laterality, follow-up time, visual acuity, and corneal thickness (in all cases $P > .05$). In addition, both groups had preoperative average topographic keratoconus classification (KC) between KC2 and KC2-3.

Digital Analysis Data

The distributions of the vectors corresponding to the steepest (peak topographic) corneal point on the preoperative map (r_p, ϑ_p) and the change map (r_d, ϑ_d) are illustrated in **Figure 2**. In the majority of the cases (more than 90%) the location of the steepest corneal point was inferior in either group.

Average radial displacement of the cone location in the cyclorotation adjusted group was 1.60 ± 0.69 mm (range: 0.57 to 3.12 mm) preoperatively; the difference maps corresponded to an average cone location at 1.39 ± 0.56 mm (range: 0.50 to 2.91 mm). The difference between preoperative and achieved change was not statistically significant ($P = .074$).

The cyclorotation adjusted group had an average value of 0.89° ± 3.28° (range: -7.5° to 9.0°); considering the absolute value of cyclorotation, the average was 2.42° ± 2.36° (range: 0.0° to 9.0)°. We were able to engage CTA in 100% of the Vario-driven cases studied. It has to be underscored that in some cases more than 30 images with the Vario were necessary to obtain reliable and feasible CTA data, a laborious process. Of the 110 eyes, 35 (32%) eyes had 0° cyclorotation (ie, below the detection limit of 0.5°), 33 (30%) eyes had between 0° and 2°, and only 8 (8%) had greater than 8°.

Average radial displacement of the cone location in the non-cyclorotation adjusted group was 1.47 ± 0.49 mm (range: 0.76 to 2.83 mm) preoperatively; the difference maps corresponded to an average cone location of 1.28 ± 0.51 mm (range: 0.46 to 2.88 mm). The difference between preoperative and achieved change in the non-cyclorotation adjusted group was also not statistically significant ($P = .067$). In addition, the preoperative cone location radial displacement between the two groups was not statistically significant ($P = .097$).

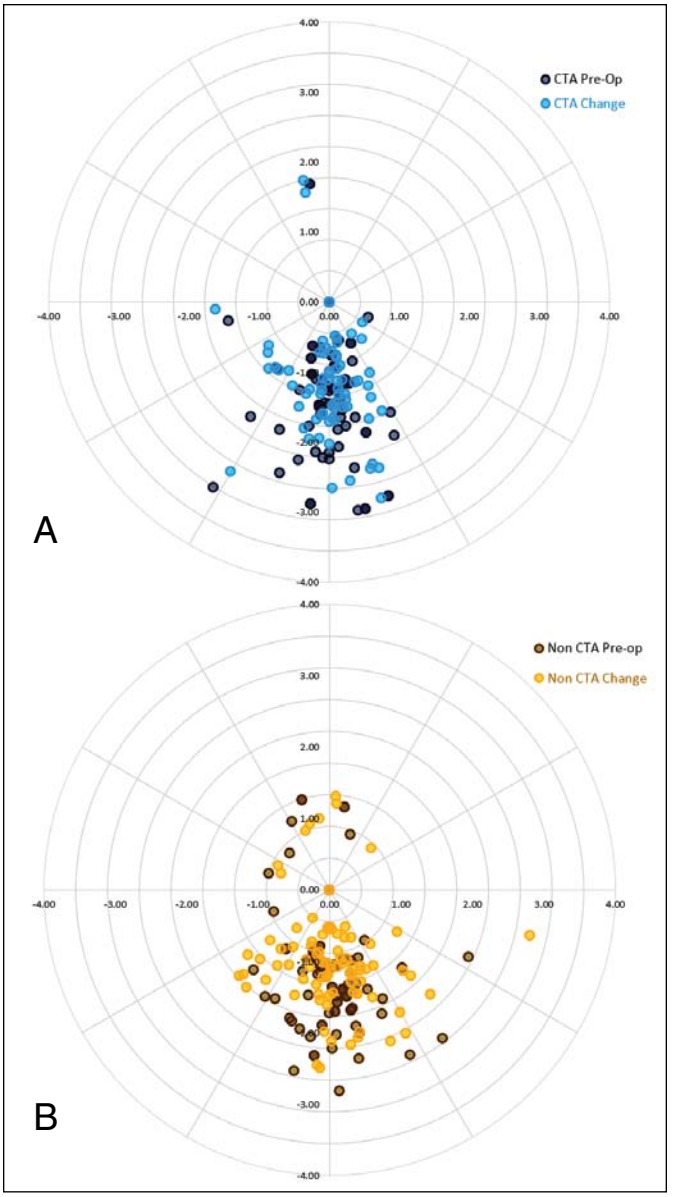

Figure 2. The distribution of the vectors corresponding to the steepest (peak topographic) corneal point on the preoperative map (r_p, ϑ_p) and the change (achieved difference) map (r_d, ϑ_d). (A) Cyclorotation adjusted and (B) non-cyclorotation adjusted groups. CTA = cyclorotational topographic adjustment

Table 1 summarizes the statistical analysis results for $\Delta\vartheta = |\vartheta_p - \vartheta_d|$, the absolute angular difference between the peak topographic angular data, and $W\Delta\vartheta = \Delta\vartheta \times \Delta r$, the weighted angular difference between the peak topographic data. The cyclorotation adjusted group had on average smaller angular difference and weighted angular difference by a statistically significant margin ($\Delta\vartheta$: $P = .0058$; $W\Delta\vartheta$: $P = .015$) compared to the non-cyclorotation adjusted group.

DISCUSSION

This study provides additional evidence for the potential of incorporating cyclorotation compensation in

TABLE 1

Statistical Analysis of Absolute Angular Difference Between the Peak Topographic Angular Data $\Delta\vartheta$ and Weighted Angular Difference $W\Delta\vartheta$

	Cyclorotation Adjusted Group			Non-cyclorotation Adjusted Group		
Parameter	$\Delta\vartheta$ (°)	$W\Delta\vartheta$ (mm)	***P***	$\Delta\vartheta$ (°)	$W\Delta\vartheta$ (mm)	***P***
Average	7.18	3.43	.0058	14.50	10.23	.0015
Standard deviation	±7.53	±4.76		±12.65	±15.15	
Minimum	0	0.00		0	0.00	
Maximum	34	21.41		49	80.56	
Confidence intervals						
0.95	±1.77	±1.12		±2.64	±3.21	
0.99	±2.35	±1.49		±3.49	±4.25	

such highly customized topography-guided treatments. We studied two large groups, which were matched preoperatively in all aspects of vision, corneal thickness, keratoconus stage, and cone location (displacement).

The Athens Protocol screening protocol involves preoperative imaging by both the Scheimpflug topometry and Placido topography devices. Either device can be synced to the operational laser planning computer on the EX500 excimer laser via a closed ethernet circuit to provide the necessary topography data. Surgeons may choose data from either device based on their own criteria. We have made it standard to review both topographies as a potential treatment and compare the treatment patterns that invariably are similar. The main difference, as far as the implementation of either treatment, is that only the Placido topography-guided treatment can employ adjunct cyclorotation adjustment, whereas the Scheimpflug-derived treatment cannot. Prior to the availability of the cyclotortional compensation option with the new Placido-imaging device (Vario), the majority of the procedures by our team adopted the Scheimpflug option, due to the improved sensitivity at the center section, when compared to the older version of Placido-produced topography employed by a predecessor device to the current Vario topographer (the Topolyzer). We have previously studied the efficacy of the Placido-derived treatments to Scheimpflug-derived treatments and with that older technology on both the topography devices (Oculyzer I vs Topolyzer) evaluated both with the 400-Hz EyeQ WaveLight excimer laser (Alcon Laboratories, Inc.) and found that the Scheimpflug-driven treatments were superior.[19]

Herein, we introduce a digital analysis technique to objectively evaluate the possible cyclotorsion effect, which may be applicable to analysis of outcomes in topography-guided treatments.

In addition to adopting cyclotortional compensation, the enhanced Athens Protocol incorporates a change in the ablation pattern sequences, by the partial PRK step preceding the PTK step. The rationale for this has been that the topography-guided ablation pattern bears the customized part, for which the active eye tracking should be performing with minimal interference. Thus, the partial-PRK step is performed first to interfere with less ablated debris and with intact epithelium for the most part providing a better image for the EX500 active tracker camera, and therefore providing the best possible pupil, iris architecture, centroid shift, and limbal anatomy imaging. The PTK step, which was initially designed to debride a uniform 50-µm thickness of epithelium over a 7-mm zone, may be performed subsequently. This rotationally symmetric PTK step does not necessitate cyclorotation compensation and is not dependent on saccadic motions to the extent of the partial PRK step.

In addition to ocular movement, there is also variable ocular rotation, known as cyclorotation or cyclotorsion. Cyclorotation affects ocular imaging and toric corrections. Cyclorotation may vary from +7.7° (excyclotorsion) to -11.0° (incyclotorsion), with a mean absolute value of 2.74° ± 2.30°.[20] Our data for cyclotorsion had an average absolute value of 2.42° ± 2.36°.

Because the majority of laser vision correction platforms incorporate custom ablation patterns, such as topography-guided or corneal wavefront ablation profiles,[21,22] accurate compensation for both movement and rotation has a major part in achieving optimal results. It would be interesting to evaluate some of these platforms with the novel methodology described herein to objectively assess perhaps equivalent, superior, or inferior accuracy.

Until recently, eye tracking with the topography-guided profile by the EX500 platform only addressed horizontal (x), vertical (y), and depth (z) movements,[23]

with limited cyclorotation compensation.[24] Even in the current configuration employed in the EX500 excimer laser, the cyclorotation compensation is static, meaning that one initial value is recorded. Thus, active cyclorotation compensation perhaps remains the last piece of the puzzle that had not been addressed until recently.[25,26]

This study indicates that incorporation of novel topography imaging technology coupled with novel excimer laser tracking technology (to include cyclorotation compensation) leads to markedly improved correlation between targeted and achieved topographic changes in the management of severely irregular corneas such as in progressive clinical keratoconus.

AUTHOR CONTRIBUTIONS

Study concept and design (AJK); data collection (AJK, GA); analysis and interpretation of data (AJK, GA); writing the manuscript (GA); critical revision of the manuscript (AJK, GA); statistical expertise (GA); administrative, technical, or material support (AJK); supervision (AJK)

REFERENCES

1. Raiskup F, Spoerl E. Corneal crosslinking with riboflavin and ultraviolet A: I. Principles. *Ocul Surf*. 2013;11:65-74.
2. Sinha Roy A, Rocha KM, Randleman JB, Stulting RD, Dupps WJ Jr. Inverse computational analysis of in vivo corneal elastic modulus change after collagen crosslinking for keratoconus. *Exp Eye Res*. 2013;113:92-104.
3. Kanellopoulos AJ. Comparison of sequential vs same-day simultaneous collagen cross-linking and topography-guided PRK for treatment of keratoconus. *J Refract Surg*. 2009;25:S812-S818.
4. Labiris G, Giarmoukakis A, Sideroudi H, Gkika M, Fanariotis M, Kozobolis V. Impact of keratoconus, cross-linking and cross-linking combined with photorefractive keratectomy on self-reported quality of life. *Cornea*. 2012;31:734-739.
5. Kanellopoulos AJ. Long term results of a prospective randomized bilateral eye comparison trial of higher fluence, shorter duration ultraviolet A radiation, and riboflavin collagen cross linking for progressive keratoconus. *Clin Ophthalmol*. 2012;6:97-101.
6. Kanellopoulos AJ, Asimellis G. Keratoconus management: long term stability of topography-guided normalization combined with high fluence CXL stabilization (the Athens Protocol). *J Refract Surg*. 2014;30:88-93.
7. Kanellopoulos AJ, Asimellis G. Introduction of quantitative and qualitative cornea optical coherence tomography findings, induced by collagen cross-linking for keratoconus; a novel effect measurement benchmark. *Clin Ophthalmol*. 2013;7:329-335.
8. Kymionis GD, Portaliou DM, Kounis GA, Limnopoulou AN, Kontadakis GA, Grentzelos MA. Simultaneous topography-guided photorefractive keratectomy followed by corneal collagen cross-linking for keratoconus. *Am J Ophthalmol*. 2011;152:748-755.
9. Stojanovic A, Zhang J, Chen X, Nitter TA, Chen S, Wang Q. Topography-guided transepithelial surface ablation followed by corneal collagen cross-linking performed in a single combined procedure for the treatment of keratoconus and pellucid marginal degeneration. *J Refract Surg*. 2010;26:145-152.
10. Kymionis GD, Grentzelos MA, Portaliou DM, Kankariya VP, Randleman JB. Corneal collagen cross-linking (CXL) combined with refractive procedures for the treatment of corneal ectatic disorders: CXL plus. *J Refract Surg*. 2014;30:566-576.
11. Tuwairqi WS, Sinjab MM. Safety and efficacy of simultaneous corneal collagen cross-linking with topography-guided PRK in managing low-grade keratoconus: 1-year follow-up. *J Refract Surg*. 2012;28:341-345.
12. Lin DT, Holland S, Tan JC, Moloney G. Clinical results of topography-based customized ablations in highly aberrated eyes and keratoconus/ectasia with cross-linking. *J Refract Surg*. 2012;28:S841-S848.
13. Siqueira JA, Dias LC, Siqueira R, et al. Longterm improvement after the Athens Protocol for advanced keratoconus with significant ectasia progression in the fellow eye. *International Journal of Keratoconus and Ectatic Corneal Diseases*. 2013;2:143-146.
14. Alessio G, L'abbate M, Sborgia C, La Tegola MG. Photorefractive keratectomy followed by cross-linking versus cross-linking alone for management of progressive keratoconus: two years follow up. *Am J Ophthalmol*. 2013;155:54-65.
15. Narváez J, Brucks M, Zimmerman G, Bekendam P, Bacon G, Schmid K. Intraoperative cyclorotation and pupil centroid shift during LASIK and PRK. *J Refract Surg*. 2012;28:353-357.
16. Tomita M, Waring GO 4th, Magnago T, Watabe M. Clinical results of using a high-repetition-rate excimer laser with an optimized ablation profile for myopic correction in 10,235 eyes. *J Cataract Refract Surg*. 2013;39:1543-1549.
17. Kanellopoulos AJ, Asimellis G. Long term bladeless LASIK outcomes with the FS200 femtosecond and EX500 excimer laser workstation: the Refractive Suite. *Clin Ophthalmol*. 2013;7:261-269.
18. Schneider CA, Rasband WS, Eliceiri KW. NIH Image to ImageJ: 25 years of image analysis. *Nat Methods*. 2012;9:671-675.
19. Kanellopoulos AJ, Asimellis G. Comparison of Placido disc and Scheimpflug image-derived topography-guided excimer laser surface normalization combined with higher fluence CXL: the Athens Protocol, in progressive keratoconus. *Clin Ophthalmol*. 2013;7:1385-1396.
20. Lucena AR, Mota JA, Lucena DR, Ferreira Sde L, Andrade NL. Cyclotorsion measurement in laser refractive surgery. *Arq Bras Oftalmol*. 2013;76:339-340.
21. Alió JL, Piñero DP, Plaza Puche AB. Corneal wavefront-guided photorefractive keratectomy in patients with irregular corneas after corneal refractive surgery. *J Cataract Refract Surg*. 2008;34:1727-1735.
22. Shaheen MS, El-Kateb M, Hafez TA, Piñero DP, Khalifa MA. Wavefront-guided laser treatment using a high-resolution aberrometer to measure irregular corneas: a pilot study. *J Refract Surg*. 2015;31:411-418.
23. Prakash G, Ashok Kumar D, Agarwal A, Jacob S, Sarvanan Y, Agarwal A. Predictive factor analysis for successful performance of iris recognition-assisted dynamic rotational eye tracking during laser in situ keratomileusis. *Am J Ophthalmol*. 2010;149:229-237.
24. Kohnen T, Kühne C, Cichocki M, Strenger A. Cyclorotation of the eye in wavefront-guided LASIK using a static eyetracker with iris recognition [article in German]. *Ophthalmologe*. 2007;104:60-65.
25. Arba-Mosquera S, Merayo-Lloves J, de Ortueta D. Clinical effects of pure cyclotorsional errors during refractive surgery. *Invest Ophthalmol Vis Sci*. 2008;49:4828-4836.
26. Wang L, Koch DD. Residual higher-order aberrations caused by clinically measured cyclotorsional misalignment or decentration during wavefront-guided excimer laser corneal ablation. *J Cataract Refract Surg*. 2008;34:2057-2062.

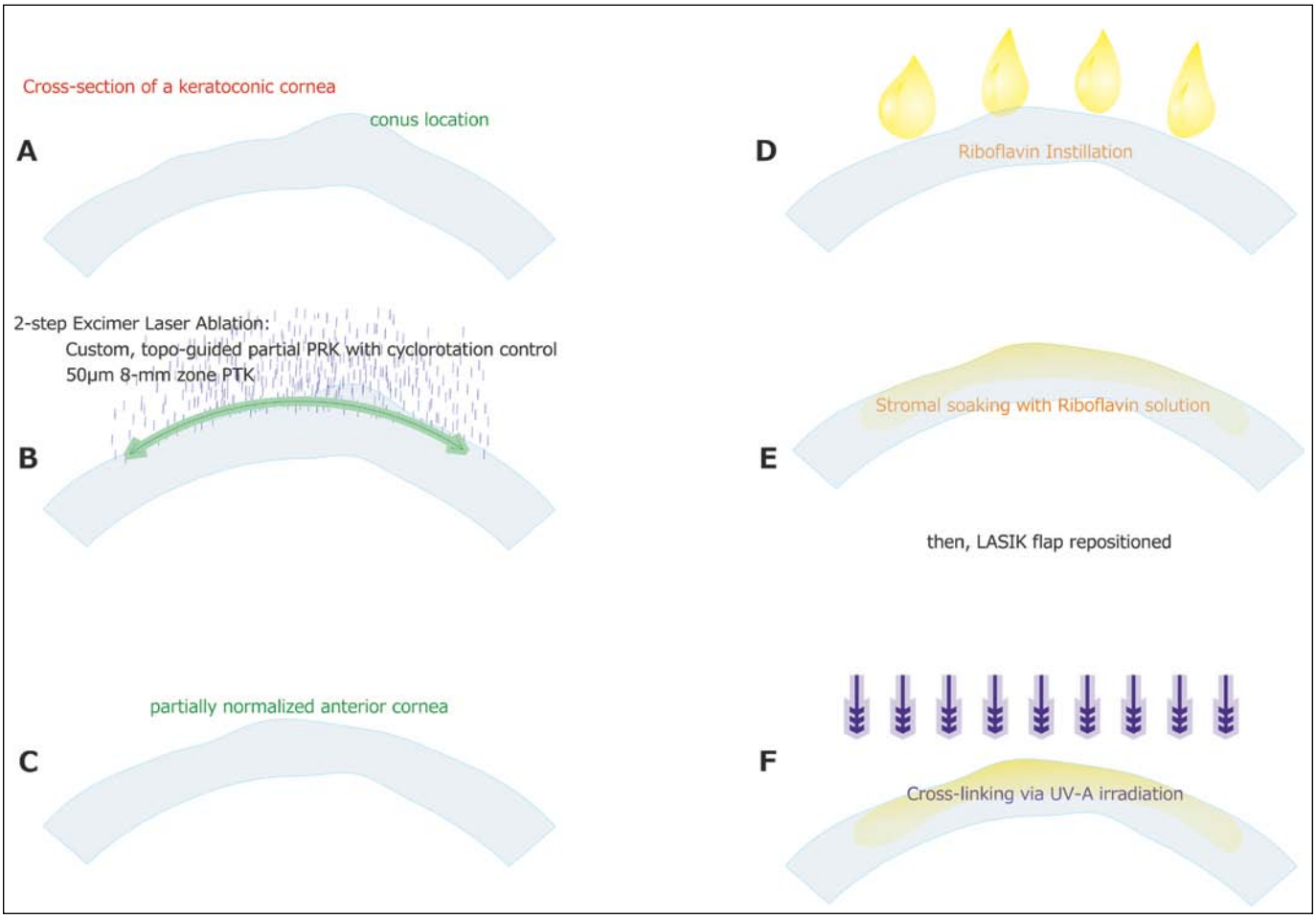

Figure A. Basic steps of the enhanced Athens Protocol procedure. (A) Import of topography-guided data to the surgical platform, (B) a two-step excimer laser ablation comprising custom topography-guided partial photorefractive keratectomy (PRK) with cyclorotation control, followed by a 50-μm deep, 8-mm optical zone diameter phototherapeutic keratectomy (PTK), (C) application of mytomicin C, (D) instillation of riboflavin, (E) stromal soaking for 80 seconds, and (F) ultraviolet-A (UV-A) irradiance of 6 mW/cm^2 applied for 15 minutes.

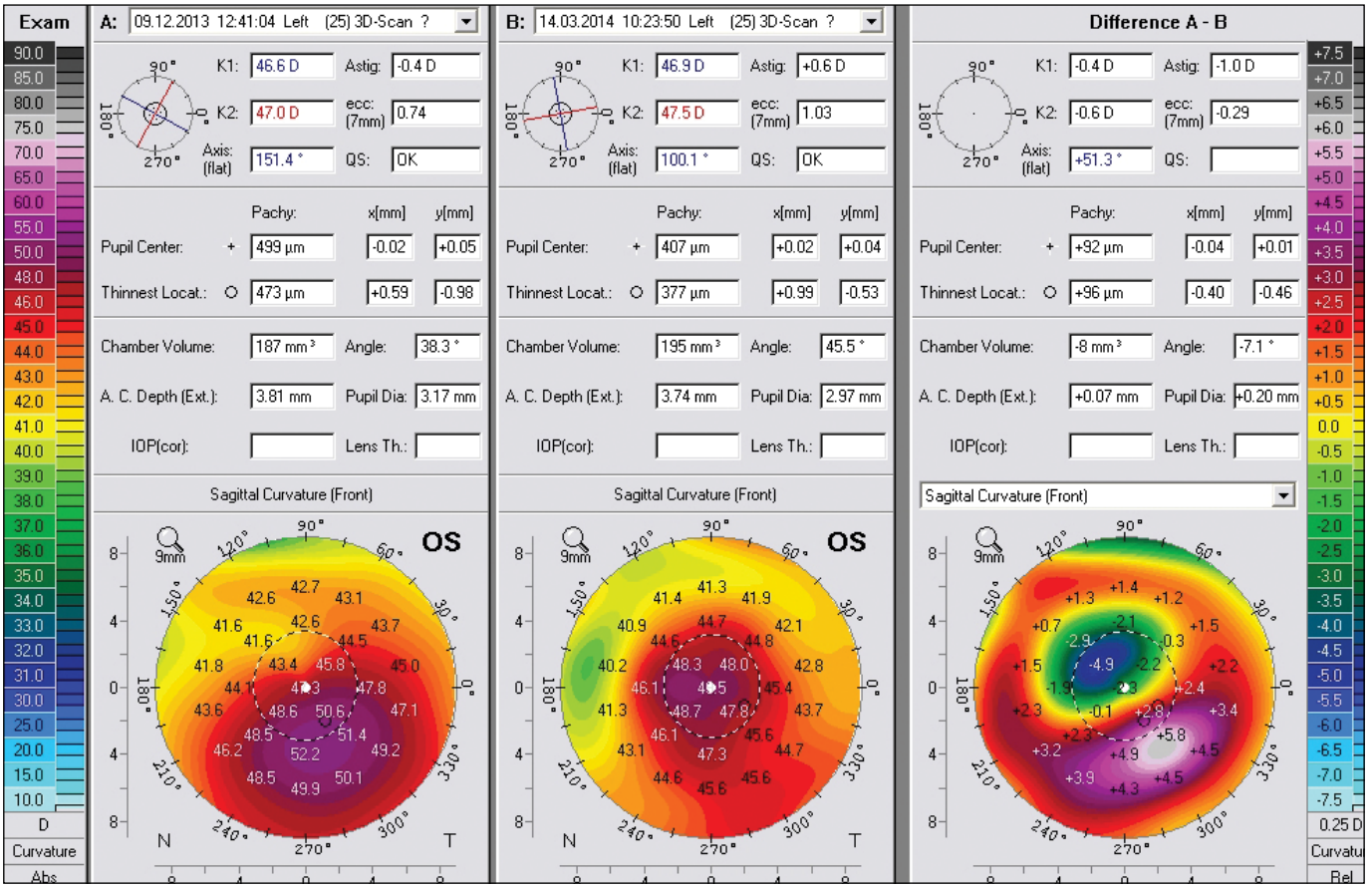

Figure B. The 'compare 2 exams' output from the Scheimpflug imaging device. (Left) The preoperative sagittal curvature map, (middle) the postoperative map, and (right) the difference of the two maps.